Journal of Chemical Crystallography, Vol. 31, No. 3, March 2001 (© 2002)

Crystal structure of tetrabutylammonium nitroprusside dihydrate, $[(C_4H_9)_4N]_2[Fe(CN)_5NO]\cdot 2H_2O$, and vibrational spectra of ground and metastable excited states of the dihydrate and the anhydrate

María E. Chacón Villalba,[1] Jorge A. Güida,[1,2] Oscar E. Piro,[3] Eduardo E. Castellano,[4] and Pedro J. Aymonino[1,5]*

Received December 18, 2000

The crystal structure of tetrabutylammonium nitroprusside dihydrate (TBANPDH, $[(C_4H_9)_4N]_2[Fe(CN)_5NO]\cdot 2H_2O$) was determined by single crystal X-ray diffraction (XRD) and the compound was also studied, as well as the anhydrous salt (TBANP), by room and low temperature Fourier Transform Infra-Red (FTIR) and room temperature Fourier Transform Near Infra-Red Raman (FTNIRR) spectroscopies. In addition to the ground states (GS), the metastable excited states (MSI and MSII) generated by laser excitation (488 nm) at low temperature were IR studied, both of the dihydrate and the anhydrate. TBANPDH crystallizes in the trigonal space group $P3_221$, D_3^6, with $a = b = 13.777(2)$, $c = 22.039(2)$ Å, and $Z = 3$. The structure was solved employing 1273 independent XR reflections, with $I > 2\sigma(I)$, by Patterson and Fourier methods and refined by full-matrix least-squares to $R1 = 0.054$.

KEY WORDS: Tetrabutylammonium nitroprusside; crystal structure; vibrational spectra; metastable states.

[1] CEQUINOR, Departamento de Química, Facultad de Ciencias Exactas, Universidad Nacional de La Plata, La Plata, República Argentina.
[2] Departamento de Ciencias Básicas, Universidad Nacional de Luján, Luján, República Argentina.
[3] IFLP and LANADI (CONICET-UNLP), Departamento de Física, Facultad de Ciencias Exactas, Universidad Nacional de La Plata, La Plata, República Argentina.
[4] Instituto de Química y Física de São Carlos, Universidade de São Paulo, São Carlos, SP, Brazil.
[5] LANEFO (CONICET-UNLP), Departamento de Química, Facultad de Ciencias Exactas, Universidad Nacional de La Plata, La Plata, República Argentina.
* To whom correspondence should be addressed at LANEFO (CONICET-UNLP), Departamento de Química, Facultad de Ciencias Exactas, Universidad Nacional de La Plata, 48 y 115, C.C. 962, 1900 La Plata, República Argentina; e-mail: aymonino@quimica.unlp.edu.ar.

Introduction

In the last 20 years, Mössbauer, infrared (IR), and Raman (R) spectroscopic results, as well as differential scanning calorimetric (DSC) and X-ray diffraction (XRD) results obtained with photogenerated excited metastable states of Fe, Os, Ru, and Ni complexes having a nitrosyl group have been reported (see Refs. 1, 2, and references therein). The most studied complex is the pentacyanonitrosylferrate(2−) anion, ($[Fe(CN)_5NO]^{2-}$), commonly named nitroprusside (NP), as the dihydrated sodium salt, $Na_2[Fe(CN)_5NO]\cdot 2H_2O$, (NaNPDH). The

1074-1542/01/0300-0155/0

isonitrosyl (FeON) structure has been proposed for MSI and a side-on, η^2-bonded geometry, Fe^{N}_{O}, for MSII, as results of very refined XRD work.[1] We recently confirmed the isonitrosyl structure of MSI from the effect of isotopic substitution on the vibrational behavior of the anion in NaNPDH.[3] To look for more information than the scarce existing in the literature[4] about the effects of a bulky cation on the formation of MSI and MSII we have studied tetrabutylammonium nitroprusside dihydrate, $[(C_4H_9)_4N]_2[Fe(CN)_5NO]\cdot 2H_2O$ (TBANPDH). The anhydrate (TBANP) was also investigated because its clearer IR spectrum (not masked by water librational bands) in the δFeCN and νFeC region (500–300 cm^{-1}).

Experimental

Preparative

TBANPDH was prepared by shaking together for 24 h, 0.03 M solutions of $(C_4H_9)_4NCl$ in chloroform and of sodium nitroprusside in water. The chloroform layer was separated and the solvent was evaporated in vacuum.[5] The solid residue was recrystallized from water by spontaneous evaporation of the solvent at room temperature. Single crystals adequate for XRD were formed. To obtain the anhydrate, the dihydrate was dried at 80°C.

Diffraction data and structure solution and refinement

As no single crystals of the anhydrate were available, single crystal XRD measurements could be performed only with the dihydrate.

Crystal data, data collection procedure, structure determination methods, and refinement of results are summarized in Table 1. As the dihydrate crystals diffracted poorly, a rather big specimen of nearly spherical shape was selected for the measurements. Despite this, only about 51% of the diffracted intensities were above two standard deviations of measurement errors. A few hydrogen atoms, including those of the water molecule, were found in a difference Fourier map. The TBA hydrogen atoms were positioned stereochemically and refined with the riding model. During the refinement, the methyl hydrogen atoms were allowed to rotate as rigid groups around the corresponding C–C bonds so as to maximize the sums of each of the electron densities at the three calculated hydrogen positions. The water H atoms were refined with O–H and H···H

Table 1. Experimental Conditions for X-Ray Diffraction

Empirical formula	$C_{37}H_{76}FeN_8O_3$
CCDC deposit no.	CCDC-1003/6018
Formula weight	736.92
Temperature	293(2) K
Crystal system	Trigonal
Space group	$P3_221$
Unit cell dimensions	$a = 13.777(2)$ Å $= b$
	$c = 22.039(2)$ Å
Volume, Å^3	3622.6(8)
Z	3
Density (calculated)	1.013 Mg/m^3
Absorption coefficient	2.789 mm^{-1}
$F(000)$	1212
Crystal size	0.5 × 0.5 × 0.5 mm
Crystal color/shape	Red/polyhedral
Diffractometer/scan	Enraf-Nonius CAD-4/$\omega - 2\theta$
Radiation, graphite monochr.	Cu Kα, $\lambda = 1.54184$ Å
Standard reflections	(0,0,15)
Decay of standard	±1.74%
θ range for data collection	3.70 to 64.91°
Reflections collected	2404
Independent reflections	2326 [$R_{int} = 0.1128$]
Observed reflects. [$I > 2\sigma(I)$]	1273
Data reduction and correction[a] and structure solution[b] and refinement[c] programs	SDP,[6] SHELX-86,[7] SHELX-93[8]
Refinement method	Full-matrix least-squares on F^2
Data/restraints/parameters	2325/0/160
Goodness of fit on F^2	1.131
Final R indices [$I > 2\sigma(I)$]	$R1 = 0.0763$, $wR2 = 0.1972$
R indices (all data)	$R1 = 0.1401$, $wR2 = 0.2653$
Absolute structure parameter	−0.02(2)
Extinction coefficient	0.0025(5)
Largest diff. peak and hole, e/Å^3	0.256 and −0.218

[a] Data were corrected for Lorentz, polarization and extinction effects.
[b] Structure solved by Patterson and Fourier methods.
[c] Neutral atomic scattering factors.

distances restrained to target values of 0.96(1) and 1.52(1) Å, respectively.

IR spectra

Nujol mulls of the substances were sandwiched between CsI disks and positioned in the sample holder of an Oxford OX8 ITL cryostat. IR spectra were obtained both at room and boiling nitrogen temperatures with a FTIR Bruker 113v spectrometer at 2 cm^{-1} resolution.

Raman spectra

Powdered samples were measured, at room temperature, with a FRA 106 Raman accessory of a Bruker IFS66 spectrometer.

Irradiation

The samples mounted in the cryostat and cooled with liquid nitrogen were irradiated with the 488 nm line of an Ar^+ # 166 Spectra Physics laser at 100 mW cm^{-2} during 5 h. Difference spectra between ground state (GS) and metastable excited states (MSI, MSII) spectra were obtained to make more evident weak bands due to the excited states.

Results and discussion

Crystallographic results for TBANPDH

Crystallographic results for TBANPDH are collected in Table 1, as already mentioned; atomic fractional coordinates of heavy atoms and equivalent isotropic temperature parameters are given in Table 2; bond distances and angles in the anion are in Table 3. In two separate tables (deposited, as supplementary, at the Cambridge Crystallographic Data Centre, CCDC) are presented, respectively, the atomic anisotropic thermal parameters and the hydrogen atoms' positions.

Table 2. Atomic Coordinates ($\times 10^4$) and Equivalent Isotropic Displacement Parameters (Å^2 $\times$ 10^3) for Tetrabutylammonium Nitroprusside Dihydrate

Atom	x	y	z	U_{eq}
Fe(1)	5643(1)	5643(1)	0	72(1)
N	6819(9)	6819(9)	0	94(3)
O	7659(8)	7659(8)	0	144(4)
C(1)	4239(11)	4239(11)	0	81(3)
N(1)	3397(9)	3397(9)	0	108(4)
C(2)	6249(7)	4791(8)	382(3)	87(2)
N(2)	6636(7)	4310(7)	605(3)	113(2)
C(3)	5193(7)	5880(7)	791(3)	85(2)
N(3)	4961(6)	6035(7)	1270(3)	108(3)
N(4)	1229(5)	4816(6)	510(3)	86(2)
C(11)	330(7)	5152(8)	434(4)	101(2)
C(12)	513(8)	5890(9)	−117(5)	120(3)
C(13)	−315(11)	6309(12)	−100(6)	159(5)
C(14)	−162(14)	7049(15)	−644(7)	220(8)
C(21)	2377(7)	5825(7)	570(3)	96(2)
C(22)	2538(11)	6615(10)	1077(4)	135(4)
C(23)	3621(13)	7678(10)	1020(5)	171(5)
C(24)	3772(15)	8473(11)	1519(6)	213(7)
C(31)	937(8)	4098(7)	1091(4)	100(3)
C(32)	1704(9)	3658(9)	1249(4)	122(3)
C(33)	1300(13)	2907(11)	1799(5)	156(5)
C(34)	252(18)	1857(17)	1712(9)	291(11)
C(41)	1240(8)	4133(8)	−27(3)	102(3)
C(42)	216(10)	3032(10)	−143(5)	152(5)
C(43)	393(17)	2428(14)	−667(7)	217(7)
C(44)	−374(28)	1390(19)	−746(12)	420(23)
O(1W)	7792(5)	3112(5)	863(2)	105(2)

U_{eq} Is Defined as One Third of the Trace of the Orthogonalized U_{ij} Tensor.

Figure 1 is an ORTEP drawing[9] of the structure showing the labelling of the non-hydrogen atoms and their displacement ellipsoids at 30% probability level. The nitroprusside ion is located on a crystallographic twofold axis. It has the well-known deformed octahedral structure, with the equatorial CN groups slightly bent toward the axial (opposite to NO) cyanide. The NCFeNO axis is exceptionally rectilinear because usually it is slightly bent (See Ref. 10 and references therein). Bond distances and angles within the NP and TBA ions are as expected from literature values,[10,11] respectively, and do not warrant further consideration. The bulky TBA cations, located at C_1 sites, look like flattened tetrahedra of about 13 Å length and contribute to keep the anions far apart,

Table 3. Bond Lengths [Å] and Angles [deg] for Tetrabutyl Ammonium Nitroprusside Dihydrate

Bond distances			
Fe(1)─N	1.620(12)	N(4)─C(31)	1.542(10)
Fe(1)─C(3)#1	1.932(8)	C(11)─C(12)	1.520(11)
Fe(1)─C(3)	1.932(8)	C(12)─C(13)	1.515(13)
Fe(1)─C(1)	1.94(2)	C(13)─C(14)	1.52(2)
Fe(1)─C(2)	1.940(10)	C(21)─C(22)	1.497(11)
Fe(1)─C(2)#1	1.940(10)	C(22)─C(23)	1.48(2)
N─O	1.157(11)	C(23)─C(24)	1.492(15)
C(1)─N(1)	1.160(14)	C(31)─C(32)	1.499(12)
C(2)─N(2)	1.148(9)	C(32)─C(33)	1.507(13)
C(3)─N(3)	1.152(8)	C(33)─C(34)	1.46(2)
N(4)─C(21)	1.500(9)	C(41)─C(42)	1.488(13)
N(4)─C(41)	1.518(9)	C(42)─C(43)	1.51(2)
N(4)─C(11)	1.533(10)	C(43)─C(44)	1.30(2)
Bond angles			
N─Fe(1)─C(3)#1	94.4(3)	N(3)─C(3)─Fe(1)	177.7(7)
N─Fe(1)─C(3)	94.4(3)	C(21)─N(4)─C(41)	108.0(6)
C(3)#1─Fe(1)─C(3)	171.3(5)	C(21)─N(4)─C(11)	111.5(7)
N─Fe(1)─C(1)	180.0(10)	C(41)─N(4)─C(11)	111.2(6)
C(3)#1─Fe(1)─C(1)	85.6(3)	C(21)─N(4)─C(31)	109.7(6)
C(3)─Fe(1)─C(1)	85.6(3)	C(41)─N(4)─C(31)	109.3(6)
N─Fe(1)─C(2)	95.0(3)	C(11)─N(4)─C(31)	107.1(6)
C(3)#1─Fe(1)─C(2)	90.3(3)	C(12)─C(11)─N(4)	113.7(6)
C(3)─Fe(1)─C(2)	89.0(3)	C(13)─C(12)─C(11)	109.3(9)
C(1)─Fe(1)─C(2)	85.0(3)	C(12)─C(13)─C(14)	111.0(11)
N─Fe(1)─C(2)#1	95.0(3)	C(22)─C(21)─N(4)	116.3(8)
C(3)#1─Fe(1)─C(2)#1	88.9(3)	C(23)─C(22)─C(21)	111.4(10)
C(3)─Fe(1)─C(2)#1	90.3(3)	C(22)─C(23)─C(24)	111.4(13)
C(1)─Fe(1)─C(2)#1	85.0(3)	C(32)─C(31)─N(4)	116.3(7)
C(2)─Fe(1)─C(2)#1	170.0(5)	C(31)─C(32)─C(33)	111.8(9)
O─N─Fe(1)	180(2)	C(34)─C(33)─C(32)	114.7(12)
N(1)─C(1)─Fe(1)	180(3)	C(42)─C(41)─N(4)	117.8(8)
N(2)─C(2)─Fe(1)	178.2(8)	C(41)─C(42)─C(43)	111.1(12)
		C(44)─C(43)─C(42)	116(2)

Note. Symmetry transformation used to generate equivalent atoms: (#1) $y, x, -z$.

at Fe─Fe distances larger than 10 Å (see below). Therefore, no appreciable correlation (Davydov) splitting between the NO groups, either electronic or vibrational, is expected—as found in other nitroprussides.[12–14]

All water molecules are crystallographically equivalent and are located at general C_1 sites and intercalated between anions presumably bridging two neighboring anions through H bonds with their equatorial cyanide nitrogen atoms.

The distances (Ow···N2) = 2.89 Å and (Ow···N3′) = 2.99 Å are among the shortest observed[15] (minimum: 2.82 Å) and the (N2···Ow···N3′) = 105.8° angle is among the greatest (maximum: 109.5°).[15] These facts suggest appreciable hydrogen bonding (see also below). It is to be mentioned that, in strontium nitroprusside tetrahydrate (SrNPTetH) the shortest Ow···N (Ow(1)···N(3)″) distance is 3.00 Å (See Ref. 16 and references therein). N(3)″ are axial nitrogen atoms. The separation between anions bonded by water is about 5 Å (Fe─Fe distances are ca. 8 Å) (cf. above).

Cooling up to boiling nitrogen temperature seems to produce no phase change either in

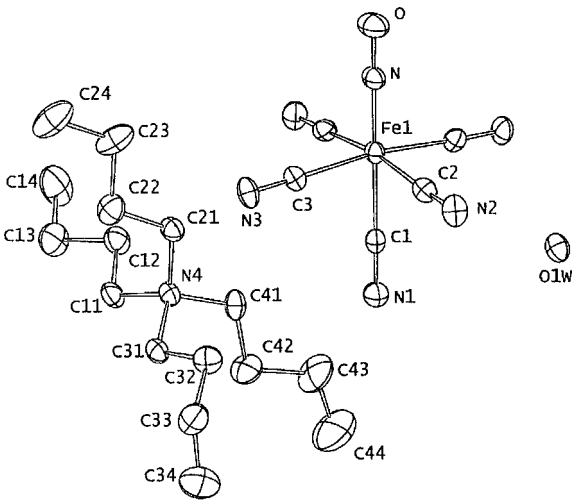

Fig. 1. ORTEP drawing of tetrabutylammonium nitroprusside dihydrate $[(C_4H_9)_4N]_2[Fe(CN)_5NO]\cdot 2H_2O$ showing the non-H atoms labeling.

TBANPDH or TBANP, as shown by IR spectroscopy (see below).

Infrared and Raman spectra of ground state TBANPDH and TBANP

The following analysis is based on results of normal coordinate analysis and Density Functional Theory calculations previously reported for the NP anion.[17]

IR and Raman spectra of ground state (GS) TBANPDH and TBANP were obtained at room temperature. IR spectra were also run at boiling nitrogen temperature, together with the respective photoexcited spectra (see below). Wave numbers and assignments of anion bands are included in Table 4. Cation bands are ignored because they do not interfere with the anion bands and are not pertinent to the purpose of this work but, anyway, CH_m ($m = 2$, 3) stretching bands appear, as expected, between 2963 and 2875 cm^{-1}, CH_m deformation bands, between 1486 and 1376 cm^{-1}, CH_m waggings and rockings, CH_2 twistings and CC stretchings between 1347 and 750 cm^{-1}, and CCC deformations at 529–522 cm^{-1}.[18]

Identification of the water bands of the dihydrate was facilitated by the comparison between IR and Raman spectra and between the IR spectra of the dihydrate and the anhydrate. Antisymmetric and symmetric OH stretching bands appear at 3501 and 3445 cm^{-1}, respectively; the deformation (scissoring) band is seen at 1665 cm^{-1}, and a band due to librations appears at 600 cm^{-1}. Figures given correspond to room temperature spectra. At boiling nitrogen temperature these bands shift to 3479, 3426, 1679, and 610 cm^{-1} and additional libration bands appear at 570 and 525 cm^{-1} together with a band at 470 cm^{-1}, which is perhaps due to a translational mode. Differences between room temperature $\tilde{\nu}$ $(OH)_{as}$, $\tilde{\nu}$ $(OH)_s$ and $\tilde{\delta}$ (H_2O) in the crystal and in the gas phase are, respectively,[19] -259, -212, and 68 cm^{-1} and with respect to liquid water, -118, -5, and 23 cm^{-1} [18] (in which case the H acceptance by O additionally lowers $\tilde{\nu}$ (OH) with respect to the decrease produced by H donation, the single effect operating in the N2$\cdots$Ow$\cdots$N3′ bridging, where water acts as H donor but not as H acceptor) confirming the H-bonding strength in the TBANPDH crystal. Interestingly, the $\tilde{\nu}$ $(OH)_{as}$, $\tilde{\nu}$ $(OH)_s$, and $\tilde{\delta}$ (H_2O) values of the abovementioned are 124 and 100 cm^{-1} below and 48 cm^{-1} above, respectively, than in NaNPDH, where the water molecules are considered to be very weakly H-bonded to CN groups.[20] The arithmetic mean value, $\bar{\tilde{\nu}}$ $(OH)_{s,\,as}$ of $\tilde{\nu}$ $(OH)_s$ and $\tilde{\nu}$ $(OH)_{as}$, is 3473 cm^{-1} for TBANPDH, a value 189 cm^{-1} smaller than the corresponding value of water diluted in CCl_4 (3662 cm^{-1}) (where H-bonding should be very weak), which is the highest of the values tabulated in Schiffer *et al.*[21] for water in organic solvents and which differs only 45 cm^{-1} from $\bar{\tilde{\nu}}$ $(OH)_{s,\,as}$ in the vapour phase (3707 cm^{-1}). In NaPDH, $\tilde{\nu}$ $(OH)_{s,\,as}$ is 3585 cm^{-1}, 112 cm^{-1} greater than in TBANPDH. In SrNPTetH, the water molecule W(1) not coordinated to the cation but H-bonded to W(3) and W(4) as acceptor, and to N(3)″ axial nitrogen as donor (the other (O)H is free), shows the $\nu(OH)_{as}$

Table 4. Wave Numbers (cm^{-1}) and Relative Intensities[a] of IR and Raman Bands of the Nitroprusside Anion in the TBANP Dihydrate and Anhydrate at Room and Low Temperature

	Dihydrate					Anhydrous				
	Room temperature		Low temperature (IR)			Room temperature		Low temperature (IR)		
Assignment[b,c]	Raman	IR	GS	MSI	MSII	Raman	IR	GS	MSI	MSII
2νNO		3758 vw	3766 vw	3507 vw			3738 vw	3746 vw	3501 vw	
νCN_{ax}			2172 sh	2161 vw		2148 s	2148 vw	2151 vw	2142 vw	
νCN	2157 vs		2163 m	2153 vw		2144 vs	2143 vw	2146 vw		
νCN			2155 m	2146 vw				2140 sh		
νCN	2150 m	2142 vs	2149 vs	2140 s		2138 m	2131 m	2134 m	2125 w	
								2111 vw		
ν^{13}CN		2118 vw	2122 vw	2112 vw			2104 vw	2107 vw	2096 vw	
ν^{13}CN		2101 vw	2105 vw	2096 vw			2088 vw	2094 vw	2082 vw	
ν^{13}CN								2091 vw		
νNO			1903 sh	1786 w	1594 vw					
νNO	1893 vw	1892 vs	1895 vs	1777 vs	1577 vw	1881 vw	1885 vs	1889 vs	1767 vs	1577 vw
ν^{15}NO		1855 vw	1858 vw	1747 vw			1845 vw	1849 vw		
$\nu N^{18}O$		1852 vw	1854 vw				1842 vw	1846 vw		
δFeNO	662 vw	662 w	665 m	580 vw		661 vw	660 vw	664 s	572 vw	
νFeN	654 w	654 w	656 w	550 vw		653 w	654 sh	656 w	535 vw	
?				502 vw			529 vw	532 vw	484 vw	
?							522 vw	522 vw	472 vw	
νFeC		497 w	502 w	485 vw			497 vw	501 vw	458 vw	
?				457 vw						
δFeCN$\perp$	456 vw	456 vw	457 w	436 vw		453 w	452 vw	454 vw		
δFeCN ||	419 vw	421 vw	425 m	420 vw			423 vw	427 m	418 vw	
?									411 vw	
νFeC		407 w	410 s	407 vw			409 sh	411 s	405 vw	
νFeC_{ax}	405 vw		405 s	401 w		402 vw		405 s	400 w	
?	395 vw	394 sh	397 w	393 vw			400 w		393 w	
νFeC	383 vw		385 w	377 vw		380 w	380 vw	385 vw	377 vw	
?						372 vw		374 vw		
νFeC								355 vw	353 vw	
δFeCN ||		318 vw	317 w	303 vw			320 vw	320 vw	303 vw	
								316 vw	290 vw	
Lattice	265 vw					264 vw				
Lattice	145 sh					149 sh				
Lattice	140 m									
δNFeC	119 m					127 s				
δNFeC	95 sh					100 m				
δNFeC	85 s					86 s				

Note. $\perp$: deformation perpendicular to the NCFeNO axis; ||: deformation parallel to it.
[a]Relative intensities: vw, very weak; w, weak; m, medium; s, strong; vs, very strong.
[b]Vibrational (symmetry) species correspond to ideal $C_{4\nu}$ symmetry of the anion.
[c]CN groups are equatorial unless otherwise (ax, axial) stated.

and $\nu(OH)_s$ bands at 3629 and 3557 cm^{-1}.[16] The mean value, 3593 cm^{-1}, is even higher than in NaNPDH, in spite of the $\tilde{\nu}$ (OH) lowering effect of the H acceptance. All these comparisons suggest that H-bonding in TBANPDH is really appreciable.

In what follows, bands due to the anion are reported and discussed.

3800–3500 region

NO overtones. The first overtone band of the NO stretching appears at 3758 and 3766 cm^{-1} in the TBANPDH room and low temperature spectra, respectively, and at 3738 and 3746 cm^{-1}, respectively, in the case of TBANP. Differences with $2\tilde{\nu}$ (NO) values, due to anharmonicities, are -26, -24 and -32, and -32 cm^{-1}, respectively. In NaNPDH and NaNP these values are -10, -20 and -21, -32 cm^{-1} respectively.[22]

2200–1800 cm^{-1} region

CN stretchings. The TBANPDH IR room temperature spectrum presents, in the $^{12}C^{14}N$ stretching region, the strongest band at 2142 cm^{-1} (see Table 4), practically at the same place as in the NaNPDH spectrum (2144 cm^{-1})[23] in spite of the fact that the H-bonding strength seems to be appreciably greater in the first case as compared with the second, as commented above. The effect of H-bonding on $\tilde{\nu}$ $(CN)_{eq}$ (the water molecules are H-bonded to the equatorial CN groups as mentioned above) should be an increasing effect[20] (see below) which seems to be compensated by the decreasing effect of the bulkier TBA cation as compared with Na^+ (again, see below).

A very weak shoulder located at 2131 cm^{-1} (not included in Table 4) could pertain to the anhydrate, which room temperature spectrum shows the strongest νCN band precisely at the same wave numbers. Traces of the anhydrate could be formed by incipient dehydration of the sample due to the dynamic vacuum kept in the optical cell and in spite that the sample is embedded in Nujol and sandwiched between CsI windows.

The strongest ν(CN) bands of the hydrate and anhydrate spectra should be related to the doubly degenerated E mode expected from the equatorial CN groups for the anion with ideal $C_{4\nu}$ symmetry (other ν(CN) bands under this symmetry are axial A_1, equatorial A_1, both IR active, and IR inactive equatorial B_1). This band should split into two nondegenerated bands under the C_2 site-symmetry in the dihydrate crystal ($C_{4\nu}$ E bands correlate with C_2 A and B bands, both types IR active) but the splitting is not seen even at low temperature.

The fact that $\tilde{\nu}$ $(CN)_{hydrate} > \tilde{\nu}$ $(CN)_{anhydrate}$ can be explained by the effect of the H-bonding in the hydrate (see above and below; also Ref. 20).

Cooling of the hydrate brings about a shoulder at 2172 cm^{-1}, which corresponds, perhaps, to the axial A_1 ($C_{4\nu}$) ν(CN) mode that in the NaNPDH low temperature spectrum appears at 2177 cm^{-1}.[24]

In the room temperature spectrum of the anhydrate two well-defined, although very weak, features appear at 2148 and 2143 cm^{-1}, more intense the first than the second (a distinction not made in Table 4 because the scale of relative intensities used involves only five steps: vw, w, m, s, vs), as expected from the axial and equatorial A_1 ($C_{4\nu}$) ν(CN) modes, respectively.

Very weak features seen at the far infrared (FIR) side of the strong ν(CN) bands of the dihydrate and the anhydrate are assigned to $^{13}C^{14}N$ groups that, due to the low natural abundance of ^{13}C, are highly diluted and do not interact vibrationally between them. Isotopic shifts are as expected by comparison with NaNPDH.[23] The three crystallographic different types of CN groups of the anions located at C_2 sites (two pairs of equivalent, opposite, groups and the axial group) should give place each to an isolated $\nu(^{13}CN)$ band, but in the hydrate spectra only two features are seen in this region at 2118 and 2101 cm^{-1} (room temperature) and at 2122 and 2105 cm^{-1} (low temperature). As the weakest of these features are those of higher wave numbers (2118 and 2122 cm^{-1}, respectively), they should correspond to the axial mode. The more intense and of lowest wave numbers bands should be due to the overlapped equatorial bands. In the $\nu(^{13}C^{14}N)$ region of the room temperature spectrum of the anhydrate also appear two features at 2104 and 2088 cm^{-1}. These bands shift to 2107 and 2091 cm^{-1} by cooling but at the same time, new, much weaker features appear at 2111 and 2094 cm^{-1}. It is tempting to consider the last band together with the 2091 cm^{-1} band as due to the two types of equatorial modes but the too different intensities

throw doubts to this interpretation. As the axial mode should not split, the 2094 cm^{-1} feature needs a different explanation.

The room temperature Raman spectrum of the dihydrate presents only two CN stretching bands, the most intense at 2157 cm^{-1} and the other at 2150 cm^{-1}. This latter band corresponds, perhaps, to the single, very strong, IR band observed in this region at 2142 cm^{-1} and assigned to the C_{4v} E mode; the first band, because its relative intensity, should be assigned to one of the A_1 modes and by comparison with the low temperature IR spectrum, to the equatorial mode (in the NaNPDH Raman spectrum this mode appears at 2162.5 cm^{-1}).[23]

The anhydrate Raman, room temperature, spectrum shows, as the IR spectrum, three features, in this case at 2148, 2144, and 2138 cm^{-1} (IR: 2148, 2143, and 2131 cm^{-1}) with relative intensities in accordance with C_{4v} A_1 axial, and equatorial A_1 and E modes.

The lower $\tilde{\nu}$ (CN) values of the anhydrous salt in comparison with the hydrate seems to be of general validity for other nitroprussides.[25] The same behavior is observed for $\tilde{\nu}$ (NO) (see next section). Interestingly, the simultaneous decreases of $\tilde{\nu}$ (CN) and $\tilde{\nu}$ (NO) have been observed for TBANP in solutions of solvents of decreasing Gutmann's acceptor number[25] (see below).

NO stretching. The very strong NO stretching band that appears, in the room temperature dihydrate IR spectrum, at 1892 cm^{-1} is shifted more than 50 cm^{-1} to lower wave numbers in comparison with the NaNPDH spectrum[23] and the shift is still greater in the anhydrous salt (room temperature spectrum), where νNO appears at 1885 cm^{-1}. These bands shift to 1895 and 1889 cm^{-1}, respectively, when cooling the samples.

Interestingly, the very weak νNO (room temperature) Raman bands are, respectively, at 1893 and 1881 cm^{-1}, practically at the same positions as in the IR spectra, proving that no vibrational interaction exists between the nitrosyl groups in the crystal lattices as expected from the big interanionic distances. This interaction is particularly strong in SrNPTetH and BaNPTriH (barium nitroprusside trihydrate) because, in the respective crystals, the NO groups are intercalated in an antiparallel way, at distances between neighbors as short as about 4 Å.[12] As a consequence of this interaction, ν(NO) shifts toward higher wave numbers when going from isolated NO groups ($^{14}N^{16}O$ in $^{14}N^{18}O$ or the reverse) to fully interacting, undiluted groups ($\tilde{\nu}$ ($^{14}N^{16}O$) of BaNPTriH is 1970 cm^{-1} and of SrNPTetH, 1968 cm^{-1}), as much as 23 cm^{-1} in the case of SrNPTetH and 21 cm^{-1} in the barium salt case. The respective stretching wave numbers of the isolated $^{14}N^{16}O$ groups are both 1947 cm^{-1}.[12] The comparison of these figures with $\tilde{\nu}$ (NO) values of TBANPDH and TBANP (1892 and 1885 cm^{-1}, respectively) suggests that, in addition to the isolating effect of the bulky TBA cations and the water molecules (see above), there is perhaps another effect,[25] i.e., a decrease of the polarization produced by the cation on the cyanide groups of the anion, with the decrease of the $d_\pi(Fe) \rightarrow \pi^*(CN)$ back-donation and the now suggested increase of the $\pi(CN) \rightarrow d_\pi(Fe)$ donation; these effects increase the $d_\pi(Fe) \rightarrow \pi^*NO$ back-donation, when going from the twice-charged M^{2+} cations to the single-charged and bulkier TBA cation. This change should also produce an increase of the σ(CN) electron population. The increase in importance of these effects with the weakening of the cation-polarizing effect should bring about, therefore, the decrease of $\tilde{\nu}$ (NO) and also of $\tilde{\nu}$ (CN), if the second of those effects surpasses the first and fourth (the effect of the decrease of the π(CN) electron density, which diminishes $\tilde{\nu}$ (CN), exceeds the combined effect of the decrease of the π^*(CN) electron density and the increase of σ(CN) population with the concomitant $\tilde{\nu}$ (CN) increase), as suggested by observation (the wave numbers of the ν(CN) strongest band in SrNPTetH and BaNPTriH spectra are 2148 and 2150 cm^{-1}, respectively, while in TBANPDH and TBANP these figures are 2142 and 2131 cm^{-1}, respectively).

In Estrin *et al.*,[25] a direct linear dependence between $\tilde{\nu}$ NO and the Gutmann's acceptor number (AN) of the solvent for TBANP dissolved

in different solvents was found, which predicts a $\tilde{\nu}$ (NO) value of 1865 cm^{-1} for zero AN. Concomitantly, $\tilde{\nu}$ (CN) also increases with increasing AN, but in a far less clear amount than $\tilde{\nu}$ (NO). The downshifts were explained as due to increasing charge transfer from the CN groups to the π*NO orbitals through the iron nucleus with the consequence of the lowering of both $\tilde{\nu}$ (NO) and $\tilde{\nu}$ (CN), although in this latter case it was supposed that a partially compensating effect is operating as a result of parallel changes in the σ(CN) and π^*(CN) electron densities. Hydrogen bonding of water with the cyanide groups should increase the $d_\pi(Fe) \rightarrow \pi^*(CN)$ back-bonding and decrease the $\pi(CN) \rightarrow d_\pi(Fe)$ donation and also, as result of these two effects, it should bring about the decrease of the $d_\pi(Fe) \rightarrow \pi^*(NO)$ back-donation with the consequence of increasing both $\tilde{\nu}$ (CN) and $\tilde{\nu}$ (NO), as discussed above.

When cooling, a shoulder appears at 1903 cm^{-1} (for very diluted samples), at the near infrared (NIR) side of the main ν(NO) band (located at 1895 cm^{-1}) of TBANPDH while this does not happen with the anhydrate. We have no explanation for this shoulder but, anyway, a phase change with the disordering of anions can be excluded as the origin of the incipient splitting because there are in the spectrum no other signals of such a change (it is to be noted that the NO group is a sensitive probe for different crystal sites as proved by the multiplicity of the stretching band observed in solid solutions of potassium nitroprusside in potassium ferrocyanide).[26]

Bands attributable to the stretching of $^{15}N^{16}O$ and $^{14}N^{18}O$ groups (present in natural concentrations) are observed about 40 cm^{-1} lower than that in the unsubstituted $^{14}N^{16}O$ anion, as expected from Chacón Villalba *et al.*[23]

700–300 cm^{-1} region

Here, and at similar positions as in the IR spectrum of NaNPDH,[17,23] the TBANPDH room temperature spectrum presents bands due to δ(FeNO) and ν(FeN), at 662 and 654 cm^{-1}, respectively. The first band is stronger than the second. These bands are shifted to 665 and 656 cm^{-1} in the low temperature IR spectrum. In the anhydrate spectra these bands appear at 660 and 654 cm^{-1} (room temperature) and 664 and 656 cm^{-1} (low temperature), respectively.

The δ(FeNO) (at 662 cm^{-1} in the dihydrate spectrum and at 661 cm^{-1} in the anhydrate spectrum) and ν(FeN) (654 and 653 cm^{-1}, respectively) Raman bands have the expected inversion of relative intensities as compared with the corresponding IR bands. The most intense are, in this case, the ν(FeN) bands ($C_{4\nu}$ A_1).

After these bands, in the IR spectra, toward the far infrared (FIR), in addition to features due to the anion, water librational bands appear in the dihydrate spectrum as mentioned above. These bands are not included in Table 4.

Because of the low Raman activity of water, the room temperature Raman spectrum of the dihydrate in this region shows no water bands.

The remaining infrared bands observed in this region are, in general, attributable mainly to FeCN bendings and FeC stretchings as suggested in Table 4. Only a few bands are of unknown origin.

300–20 cm^{-1} region

This region was explored only with Raman spectroscopy at room temperature. Between 265 and 140 cm^{-1} bands attributable to lattice vibrations appear, while bands located between 127 and 85 cm^{-1} are assigned mainly to skeletal $\delta(XFeY)$ vibrations ($X = N$, $Y = C$, and $X = Y = C$) of the anion.

Excited states

Infrared spectra at 77 K. The irradiation of nitroprussides at low enough temperatures generates two metastable states, MSI and MSII, a series of salts for which decay temperatures are around 197 and 141 K (mean values), respectively,[4] but the respective values for TBANPDH and TBANP are between 170–180

and 100–120 K. These values are lower than most of the reported values,[4] among which, the nearest values are 180 K for $[Na(18\text{-crown-}6)]_2\,NP{\cdot}8H_2O$ (see ref. 1(c) and references therein) and 128 K for $(CN_3H_6)_2NP$, respectively. This limit (180 K) is the MSI decay temperature of $[Na(18\text{-crown-}6)]_2[Fe(CN)_5NO]{\cdot}8H_2O$ (See Ref. 1(c) and references therein). For $[(CH_3)_4N]_2NP{\cdot}xH_2O$ only the MSI decay temperature is reported (at 186 K) not far from the higher limit of the range found for the TBA salts. Interestingly, the single MS found for (cubic) $FeNP{\cdot}xH_2O$ decays at about 250 K.[27] The relatively low decay temperatures of MSI and MSII in the TBA salts could be explained as due to their soft structures, which facilitate the rearrangement of the photoisomers to the GS configuration.[1] The high value reported for the decay of excited $FeNP{\cdot}xH_2O$ could be explained by the polarizing effect on the anions exercised by the Fe^{2+} cation bonded to them through the N ends of the CN groups (see above) (for the crystal structure of $FeNP{\cdot}2H_2O$).[28]

As advanced above, difference spectra were useful to detect excited states bands. The shifts of these bands with respect to the GS bands have been explained as due to the relaxation of bonds and the isomerization of the FeNO group to the lineal FeON structure for MSI and the sideway, η^2-bonded Fe^{N}_{O} geometry for MSII upon excitation, as mentioned above.[1,2]

Bands observed are included in Table 4 but more bands than seen should appear in the spectra. Too weak bands do not appear due to the relatively low concentration of excited states achieved, always far below the upper limit of 50%).[1]

3510–3500 cm^{-1} region

Only MSI ν(NO) first overtone (2ν(NO)) appears at 3507 and 3501 cm^{-1} in the dihydrate and anhydrate spectra, respectively (Table 4). Differences between $\tilde{\nu}$ (2ν(NO)) and $2(\tilde{\nu}$ (NO)) are -47 and -33 cm^{-1}, respectively, indicating that the anharmonicity shift of MSI ν(NO) is nearly double that of GS ν(NO) in the dihydrate (-24 cm^{-1}) while, surprisingly, in the anhydrate both are practically the same (32 cm^{-1} for GS) (in NaNPDH the anharmonicity shifts of GS and MSI ν(NO) are -20 and -35 cm^{-1} [22] and in NaNP, -32 cm^{-1} [22] for the GS while the overtone band has not been observed for MSI). The shift as high as -47 cm^{-1} remains, therefore, to be explained.

2200–1500 cm^{-1} region

CN stretching bands of excited TBANP dihydrate and anhydrate, four and two, respectively, for MSI (but none observed for MSII), are also at lower wave numbers (relaxed) in comparison with GS bands (shifts are ca. -10 cm^{-1}) as it happens with sodium and barium nitroprussides, among other nitroprussides.[3,29–31] This fact could be explained by an increase in the $\pi(CN) \rightarrow d_\pi(Fe)$ donation and a decrease of the $d_\pi(Fe) \rightarrow \pi^*(CN)$ back-donation upon excitation, which overcompensates the $d_\pi(Fe) \rightarrow \pi^*(ON)$ back-donation, increasing the electron density on the (Fe) nucleus of the complex anion and, therefore, decreasing its formal oxidation number (see below).

In the $\nu(^{13}CN)$ region, two MSI bands appear in both the dihydrate and the anhydrate spectra displaced again about -10 cm^{-1}.

Shifts of ν(NO) bands are -118 and -318 cm^{-1} for MSI and MSII, respectively, for the dihydrate and -122 and -312 cm^{-1}, respectively, for the anhydrate. It is to be remembered that the relative shifts suffered by ν(NO) bands upon excitation are used to identify the excited states because the less shifted ν(NO) is assigned to MSI, and the most to MSII.[1] For NaNPDH, shifts of ν(NO) are 112 and 283 cm^{-1} and for $FeNP{\cdot}xH_2O$, 113 and 204 cm^{-1} for MSI and MSII, respectively.[27]

It is to be noted that the large ν(NO) shifts seemed to be not supported by corresponding NO bond length increases that were very small, if observed at all, for NaNPDH[1], but recently, an NO bond elongation has been found for MSI of *trans*-$[Ru(en)_2(H_2O)(NO)]^{3+}$,[32] in accordance with the ν(NO) downshift.

Interestingly, shifts are larger when TBA is the cation than when the cation is monoatomic, a

difference that could be explained again by the differences in packing densities (it is a well-known fact that densification of a crystal structure as brought about by cooling or external pressure increase, leads to a compression of the interatomic bonds of the polyatomic components of the crystal, stiffening the bonds and, therefore, increasing the vibrational wave numbers).

700–300 cm^{-1} region

TBANPDH provides, upon irradiation, relatively more intense MSI bands than NaNPDH in this region, making, therefore, easier to detect weak bands and to make assignments. On the contrary, no MSII bands were observed in this region and below it either in the hydrate or the anhydrate spectra.

The MSI δ(FeON) and ν(FeO) modes (we are considering that the anion in MSI has an isonitrosyl structure) appear in the TBANPDH spectrum as two very weak IR bands located at 580 and 550 cm^{-1}, respectively, while the corresponding bands could not be observed for MSII, as advanced above. In the TBANP spectrum, those MSI bands appear at 572 and 535 cm^{-1}. Below these last wave numbers MSI bands are, in general, very weak with the exception of the band at 401 cm^{-1} of the dihydrate, which is of weak relative intensity.

Again, in excited NaNPDH spectra, the region between 430 and 320 cm^{-1} is much less defined than in the present case and precisely, present results were very helpful in assigning bands in this region for excited NaNPDH.[3]

Conclusions

TBANPDH crystallizes in the trigonal space group $P3_221$, D_3^6. $a = b = 13.772(2)$, $c = 22.039(2)$ Å, $Z = 3$. The anions are located at C_2 sites and presumably H-bonded to the water molecules through the equatorial cyanide groups. The cations and the water molecules are in C_1 sites. Cooling seems to bring no phase change, as it seems also to be the case for TBANP, the structure of which could not be determined due to the lack of single crystals. The bulky TBA cations and the water molecules keep the anions far apart so as to avoid vibrational interaction between them, and the low polarization power of the cations allows the increase of $\pi(\mathrm{CN}) \rightarrow \mathrm{d}_\pi\mathrm{Fe}$ and $\mathrm{d}_\pi\mathrm{Fe} \rightarrow \pi^*\mathrm{NO}$ donations with the concomitant softening of the CN and NO bonds, respectively. The softening is much increased by photoexcitation, which leads to metastable I and II states (MSI, MSII) to which the FeON and Fe^N_O structures are assigned, respectively.[1,3] Decay temperatures are decreased in comparison with monatomic-cation nitroprussides, a fact that could be due to the more open and soft structures of the TBA salts that facilitate the thermal rearrangement of the excited FeON (MSI) and Fe^N_O(MSII) structures to the GS FeON structure.[1]

Acknowledgments

To the reviewers for helpful suggestions to improve the manuscript. M.E.C.V., J.A.G., and P.J.A. are thankful to CONICET and CICPBA for financial support through CEQUINOR, to CONICET for the grant PIP # 4752, to ANPCyT for PICT # 06-00005-00118, and to UNLP, for support to a research incentive program. J.A.G. also thanks partial support from Universidad Nacional de Luján; O.P. acknowledges financial help from CONICET and E.E.C. from Fundãçao Vitae, Brazil.

References

1. (a) Coppens, P.; Fomitchev, D.; Carducci, M.D.; Culp, K. *J. Chem. Soc. Dalton Trans.* **1998**, 865. (b) Fomitchev, D.V.; Coppens, P. *Comments Inorg. Chem.* **1999**, *21*, 131. (c) Fomitchev, D.V.; Navozhilova, I.; Coppens, P. *Tetrahedron* **2000**, *56*, 6813.
2. Schaiquevich, P.S.; Güida, J.A.; Aymonino, P.J. *Inorg. Chim. Acta* **2000**, *303*, 277.
3. Chacón Villalba, M.E.; Güida, J.A.; Varetti, E.L.; Aymonino P.J. *Spectrochim. Acta* **2000**, *A57*, 367.
4. Zollner, H.; Krasser, W.; Woike, Th.; Haussühl, S. *Chem. Phys. Lett.* **1989**, *161*, 497.
5. Manoharan, P.T.; Gray, H.B. *J. Am. Chem. Soc.* **1965**, *87*, 3340.
6. Frenz, B.A. *Enraf-Nonius Structure Determination Package*; Enraf-Nonius: Delft, The Netherlands, 1983.
7. Sheldrick, G.M. *Acta Cryst.* **1990**, *A46*, 467.

8. Sheldrick, G.M. *SHELXL93, Program for Crystal Structure Refinement*; University of Göttingen: Germany, 1993.
9. Johnson, C.K. ORTEP; Report ORNL-3794, Oak Ridge, TN, 1965.
10. (a) Soria, D.B.; Piro, O.E.; Castellano, E.E.; Aymonino, P.J. *J. Chem. Crystallogr.* **1999**, *29*, 75. (b) Bottomley, F.; White, P.S.; *Acta Cryst.* **1979**, *835*, 2193.
11. Homoloya, L.; Preetz, W. *Z. Naturforsch.* **1999**, *B54*, 1009.
12. (a) González, S.R.; Aymonino, P.J.; Piro, O.E. *J. Chem. Phys.* **1984**, *81*, 625. (b) González, S.R.; Piro, O.E.; Aymonino, P.J.; Castellano, E.E. *Phys. Chem. Rev. B* **1986**, *33*, 5818.
13. Güida, J.A.; Piro, O.E.; Aymonino, P.J.; Sala, O. *J. Raman Spectrosc.* **1992**, *23*, 131.
14. Benavente, A.; de Morán, J.A.; Piro, O.E.; Castellano, E.E.; Aymonino, P.J. *J. Chem. Crystallogr.* **1997**, *27*, 343.
15. Chiari, G.; Ferraris, G. *Acta Cryst.* **1982**, *B38*, 2331.
16. (a) Navaza, A.; Chevrier, G.; Gukasov, A.; Aymonino, P.J. *J. Solid State Chem.* **1996**, *123*, 48. (b) Aymonino, P.J.; Rivero, B.E.; Castellano, E.E. *J. Mol. Struct.* **1981**, *70*, 241.
17. Chacón Villalba, M.E.; Varetti, E.L.; Aymonino, P.J. *Spectrochim. Acta* **1999**, *55*, 1545.
18. Lin-Vien, D.; Colthup, N.B.; Fateley, W.G.; Grasselli, J.G. *The Handbook of Infrared and Raman Characteristic Frequencies of Organic Molecules*; Academic Press: San Diego, CA, 1991; pp. 9–11.
19. Nakamoto, K. *Infrared and Raman Spectra of Inorganic and Coordination Compounds*; Wiley: New York, 1997.
20. Holzbecher, M.; Knop, O.; Falk, M. *Can. J. Chem.* **1971**, *49*, 1413.
21. Schiffer, J.; Intenzo, M.; Hayward, P.; Calabrese, C. *J. Chem. Phys.* **1976**, *64*, 3014.
22. Chacón Villalba, M.E.; Güida, J.A.; Varetti, E.L.; Aymonino, P.J. To be reported elsewhere.
23. Chacón Villalba, M.E.; Varetti, E.L.; Aymonino, P.J. *Vib. Spectrosc.* **1997**, *14*, 275.
24. Güida, J.A.; Aymonino, P.J.; Piro, O.E.; Castellano, E.E. *Spectrochim. Acta* **1993**, *49A*, 535.
25. Estrin, D.A.; Baraldo, L.M.; Slep, L.D.; Barja, B.C.; Olabe, J.A. *Inorg. Chem.* **1996**, *35*, 3897.
26. González, S.R.; Aymonino, P.J.; Mercader, R.; Piro, O.E. *J. Phys. Chem. Solids.* **1986**, *47*, 239.
27. Morioka, Y.; Hisamitsu, T.; Inoue, H.; Yoshika, N.; Tomizawa, H.; Miki, E. *Bull. Chem. Soc. Jpn.* **1998**, *71*, 837.
28. Mullica, D.F.; Tippin, D.B.; Sappenfield, E.L. *J. Crystallogr. Spectrosc. Res.* **1991**, *21*, 81.
29. Güida, J.A.; Aymonino, P.J. *Solid State Commun.* **1986**, *57*, 175.
30. Güida, J.A.; Aymonino, P.J.; Piro, O.E.; Castellano, E.E. *Spectrochim. Acta* **1993**, *49A*, 535.
31. Güida, J.A.; Piro, O.E.; Aymonino, P.J. *Solid State Commun.* **1988**, *66*, 1007.
32. Kawano, M.; Ishikawa, A.; Morioka, Y.; Tomizawa, H.; Miki, E.; Ohashi, Y. *J. Chem. Soc. Dalton Trans.* **2000**, 2425.